AIAA JOURNAL
Vol. 32, No. 2, February 1994

Nonlocal Thermodynamic Equilibrium in Laser-Sustained Plasmas

David K. Zerkle* and Herman Krier†
University of Illinois at Urbana-Champaign, Urbana, Illinois 61801

An argon laser-sustained plasma at atmospheric pressure has been studied spectroscopically and the existence of a nonlocal thermodynamic equilibrium state has been determined. The spectroscopic data consist of argon-neutral and -ion line emissions used to spatially resolve electronic energy level population densities in each plasma species. A hydrogen seed is added to the argon flow for the purpose of determining electron number density by Stark broadening analysis of the Balmer series alpha line. Electron and heavy particle kinetic temperatures are calculated through the use of an appropriate nonequilibrium model. The dominant nonequilibrium effect in this plasma is kinetic nonequilibrium where the electron kinetic temperature can be more than twice the heavy particle kinetic temperature in high laser power flux regions. Typical electron and heavy particle kinetic temperatures are 14,000 K and 8000 K, respectively. Electron number density ranges from 6×10^{16} cm^{-3} to 2.1×10^{17} cm^{-3}.

Nomenclature

E_H = hydrogen ionization potential
E_i = electronic energy of level i
E_{Ia} = lowered neutral ionization potential
g_i = electronic degeneracy of level i
H_α = hydrogen Balmer series alpha line
h = Planck's constant
k_b = Boltzmann's constant
M = heavy particle mass
m_e = electron mass
n_a = neutral particle number density
n_e = electron number density
n_e^* = critical n_e for Boltzmann equilibrium
n_i = ion number density
n_m = population of electronic energy level m
T_e = electron kinetic temperature
$T_{ex\beta,n}$ = upper-level electronic excitation temperature of species n
T_{exn} = total electronic excitation temperature of species n; relates population of highest excited level to ground level
T_g = heavy particle kinetic temperature
T_{LTE} = temperature due to a local thermodynamic equilibrium line emission analysis
Z_{exn} = electronic partition function of species n
$\epsilon(r)_L$ = radial line emission coefficient

Introduction

LASER-SUSTAINED plasmas have been proposed as the mechanism by which laser energy is converted into the thermal energy of a propellant for use in space propulsion applications.[1,2] For this laser propulsion system to be successful for space applications, it is important that the system absorb all or nearly all of the incident laser energy and retain as much of it as possible in the form of thermal energy of the plasma exhaust gas. A number of experimental investigations aimed at measuring the global energy conversion performance of laser-sustained plasmas (LSPs) have been undertaken.[3-6]

To this end a detailed understanding of the absorption and subsequent conversion processes is of the utmost importance. The character and relative importance of plasma energy conversion and transport mechanisms depends directly on the thermodynamic state of the plasma propellant gas. Plasma constituent particle temperatures and densities are key elements in the thermodynamic description of the LSP, and are the focus of this investigation.

In a plasma environment it is often assumed that local thermodynamic equilibrium (LTE) exists. This assumes that all the energy modes in the plasma gas, both electronic and kinetic, are governed by a single equilibrium temperature. Due to the large external radiation field applied by the laser, and strong temperature and density gradients within the plasma, this LTE assumption is not valid all the time. In a non-LTE state constituent particle number densities cannot be determined in the straightforward manner familiar to LTE plasma analyses.

The main objective of this paper is to demonstrate the existence and extent of various non-LTE effects in laser-sustained plasmas. The weaknesses of LTE spectroscopic analysis are pointed out, as are some advantages of this analysis when applied to this plasma. A comparison is made to the results of an LTE numerical model[7] employed to simulate this plasma. The weaknesses of the model which result in its poor prediction of the local plasma thermodynamic state are discussed.

To undertake a non-LTE plasma investigation some plasma emission measurements must be made and used in conjunction with an appropriate thermodynamic model. In this investigation a flowing argon plasma with a trace of hydrogen is sustained at atmospheric pressure by 5 kW of CO_2 laser power. Spectroscopic measurements of several argon-neutral and -ion emission lines are made in both the axial and lateral dimensions. A similar measurement is made of the hydrogen Balmer series alpha line profile for the purpose of electron number density determination through Stark broadening theory. The important quantities resulting from this non-LTE argon LSP investigation are T_e and T_g (all heavy particles are assumed to be in kinetic equilibrium due to their nearly equivalent atomic masses), n_e, n_a, T_{exa}, and T_{exi}.

The primary mechanism whereby laser radiation is absorbed by the plasma is called inverse bremsstrahlung (IB). In the IB

Presented as Paper 92-2991 at the AIAA 23rd Plasmadynamics and Lasers Conference, Nashville, TN, July 6–8, 1992; received July 28, 1992; revision received July 23, 1993; accepted for publication Aug. 17, 1993. Copyright © 1993 by the American Institute of Aeronautics and Astronautics, Inc. All rights reserved.

*Graduate Research Assistant, Department of Mechanical and Industrial Engineering; current address, Los Alamos National Laboratory, Chemical Science and Technology Division, Los Alamos, NM 87545. Member AIAA.

† Professor, Department of Mechanical and Industrial Engineering. Fellow AIAA.

process free electrons in the presence of atoms or ions absorb laser photons and gain kinetic energy. Through collisional processes with the heavy particles the entire gas becomes heated. If the input laser power flux is great enough to overcome electron recombination and other electron energy losses, the heating and subsequent ionization will continue until the LSP stabilizes in the vicinity of the laser focus.

LTE implies that electron collisions wholly determine the state of matter within the plasma. The laws of Maxwell, Boltzmann, and Saha can be used in LTE to determine the plasma composition with a temperature equal to T_e. The electron density at which LTE holds is not known precisely for all cases, and care must be taken before it is assumed. It is best to undertake a study of laboratory plasmas without assuming LTE and then later determine if such an assumption might be valid for similar cases. Several criteria on electron number density have been proposed for the establishment of LTE in plasmas. The criteria for kinetic equilibrium and Boltzmann equilibrium are of particular importance to this work.

Kinetic nonequilibrium implies that the electron kinetic temperature is not the same as the heavy particle kinetic temperature. It arises when an external field is applied to the plasma. The mobility of the electrons is much higher than that of the heavy particles, and so the bulk of the absorbed laser energy is transferred to the electrons. In other words the IB laser absorption process increases the kinetic energy of the electrons much more than it does the heavy particles in the electron-photon-heavy particle three-body collision.

Laser irradiance (W/m^2) can be expressed in terms of the amplitude of its electric field vector (V/m) by the following:

$$I = \frac{ce_0}{2} E_0^2 \tag{1}$$

For a laser power of 5 kW giving a modest irradiance estimate of 10^8 W/m^2 the electric field amplitude is 2.7×10^5 V/m. Griem[8] gives a criterion for kinetic equilibrium based on the amount of energy absorbed by the electrons and the amount transferred to the heavy particles through elastic collisions. The expression is given in terms of the external electric field strength:

$$E^2 \ll \left[5.5 \times 10^{-12} n_e \frac{E_H}{k_b T_e} \right]^2 \frac{m_e}{M} \tag{2}$$

where E_H and $k_b T_e$ are expressed in eV, and n_e is in cm^{-3}. For an equilibrium composition of argon at one atmosphere the maximum electron density is $\sim 2 \times 10^{17}$ cm^{-3} at 16,700 K. The right-hand side of inequality (2) is 1.5×10^9 for these conditions and the criterion is failed by at least two orders of magnitude. Therefore it is reasonable to expect kinetic nonequilibrium in laser-sustained argon plasmas.

If Boltzmann equilibrium holds, then the ground-level population densities of plasma atomic particles can be determined from the measurement of excited-level population densities. This leads directly to the number densities of the corresponding particles.

A criterion given by Drawin[9] gives the electron number density required for a Boltzmann distribution to extend to the ground level of an atom. The expression for critical electron number density is (cm^{-3}):

$$n_e^* \geq 6.5 \times 10^{10} \frac{g_p}{g_q} (E_p - E_q)^3 \sqrt{T_e}\, \Phi_j(X_{pq}) \tag{3}$$

where levels p and q are the furthest separated in energy in the atom, X_{pq} is a parameter defined as $(E_p - E_q)/k_b T_e$, and Φ_j is given as a function of X_{pq} by Drawin. The neutral species corresponds to $j = 1$, and $j = 2$ indicates singly charged ions. The energies must by given in eV and the temperature in Kelvin. For a typical argon electron kinetic temperature found in the LSP studied here, say $T_e = 14{,}000$ K, and using the ground ($q = 1$) and first excited ($p = 2$) levels of argon-neutral and -first-ion, the quantities in Table 1 are determined from Drawin and the preceding criterion.

Table 1 Critical electron densities, n_e^*

	Neutral	Ion
g_1	1	4
g_2	3	2
E_1	0	0
E_2	11.623	13.480
X_{pq}	9.634	11.173
Φ_j	10.601	3.031
n_e^*, cm^{-3}	3.84×10^{17}	2.85×10^{16}

As will be shown in the results of this work, the lowest measured electron number density in the LSP is approximately 6×10^{16} cm^{-3}, and the highest approximately 2×10^{17} cm^{-3}. So it seems that the ions should be in Boltzmann equilibrium, but the neutrals should not. However, the preceding criterion assumes that there are no factors at work to destroy equilibrium other than the escape of optically thin line radiation, and that collisions between plasma particles are the only means of maintaining equilibrium. The situation is actually more complicated due to the entrapment of resonance radiation which tends to enhance equilibrium by reducing the overpopulation of the ground state.

The effect trapping of resonance radiation has on critical electron number density is treated by Griem.[8] He states that the critical density may be reduced by a factor of 10 if the following condition is met:

$$n_1 d > 8 \times 10^{10} \left[\frac{E_2 - E_1}{f_{12}} \right] \left[\frac{T_e}{M_a} \right]^{1/2} \tag{4}$$

where n_1 is the population of the ground level, d is the thickness of the plasma in centimeters, f_{12} is the oscillator strength of the resonance transition, and M_a is the atomic mass number of the particle considered. For argon-neutral $f_{12} = 0.061$, and for the ion $f_{12} = 0.0089$ (see Ref. 10). Taking $d = 1$ cm, which approximates the LSP diameter, and $M_a = 40$, the ground-state population of neutrals must be at least 2.8×10^{16} cm^{-3}, and that of the ions at least 2.3×10^{15} cm^{-3} for the criterion to be satisfied. These populations are easily met in the LSP studied in this investigation.

The previous discussion indicates that the resonance radiation trapped by the argon-neutral particles may reduce n_e^* to as low as 3.84×10^{16} cm^{-3}, which is achieved in this LSP. It may then be expected that both the ionic and neutral argon electronic systems be in Boltzmann equilibrium. This condition will be assumed for the neutral system in this investigation so that neutral particle number density can be reliably approximated.

In this investigation diagnostic techniques are applied which are independent of an explicit LTE assumption. These techniques follow those of Eddy and Sedghinasab,[11] Eddy,[12] and Cho[13] who work mainly with electric arc-driven plasmas and plasma jets, and will incorporate terminology found in their work as it has proved quite applicable to LSP diagnostics.

Common to most non-LTE thermodynamic models are the use of Boltzmann factors, an equation of state, and some type of ionization equation. It is the form of the ionization equation which separates one model from the next, and it is the physical system to which the model is applied that determines the appropriate form of this equation.

When various nonequilibrium effects are present, such as nonequivalence of the electron and heavy particle kinetic temperatures, or nonequivalence of the electronic excitation temperatures and the electron kinetic temperature, then the ionization equation takes on different forms depending on the types of nonequilibrium to be considered. A general form of the law of mass action describing the relationship among

plasma particle number densities for an ionization reaction is due to Potapov,[14] and is written as:

$$\prod_j n_j^{\nu_j k_b T_{jt}} = e^{-\sum_j \nu_j E_{0,j}} \prod_j \times \left[\left(\frac{2\pi m_j k_b T_{jt}}{h^2} \right)^{\nu_j (3/2) k_b T_{jt}} \prod_{k>1} Z_{jk}^{\nu_j k_b T_{jk}} \right] \tag{5}$$

where ν_j is the stoichiometric coefficient of species j in the ionization reaction, T_{jt} is the kinetic temperature of species j, $E_{0,j}$ is the zero-point energy of species j, and T_{jk} is the temperature used in the calculation of Z_{jk}, the partition function for mode k of species j.

For the ionization of a monatomic gas in chemical equilibrium, Eq. (5) reduces to:

$$n_e \left(\frac{n_i}{n_a} \right)^{T_g/T_e} = 2 \frac{Z_{\mathrm{exi}}^{(T_{\mathrm{exi}}/T_e)}}{Z_{\mathrm{exa}}^{(T_{\mathrm{exa}}/T_e)}} \left(\frac{2\pi m_e k_b T_e}{h^2} \right)^{3/2} \exp\left(\frac{-E_{Ia}}{k_b T_e} \right) \tag{6}$$

where the kinetic temperatures of the neutral atoms and ions are assumed equal to a gas temperature T_g, and T_{exa} and T_{exi} are used in the calculation of Z_{exa} and Z_{exi}, respectively.

The above ionization equation is the one used in this paper. Its main features are that it allows for 1) kinetic nonequilibrium between the electron and the heavy particles, $T_e \neq T_g$, 2) electronic excitation nonequilibrium between the electrons and the neutral atoms, $T_e \neq T_{\mathrm{exa}}$, and 3) between the electrons and the ions, $T_e \neq T_{\mathrm{exi}}$.

An alternative expression for the ionization equation was proposed during the technical review of this article by Martinez-Sanchez.[15] It is of the form:

$$n_e \left(\frac{n_i}{n_a} \right) = 2 \frac{Z_{\mathrm{exi}}}{Z_{\mathrm{exa}}} \left(\frac{2\pi m_e k_b T_e}{h^2} \right)^{3/2} \exp\left(\frac{-E_{Ia}}{k_b T_e} \right) \tag{7}$$

where Z_{exa} and Z_{exi} are evaluated at T_{exa} and T_{exi}, respectively. The main difference between Eqs. (6) and (7) is that there is no dependence on T_g in Eq. (7). The derivation of Eq. (6) is based on the minimization of Gibbs free energy, whereas Eq. (7) results from the maximization of entropy. According to Martinez-Sanchez, the Gibbs free energy is not minimized at chemical equilibrium in a multitemperature system.

As far as this work is concerned, the application of Eq. (7) rather than Eq. (6) does not affect the final plasma temperatures calculated to any significant extent. For example, the greatest kinetic nonequilibrium is found near the plasma front, where $T_e = 13{,}964$ K and $T_g = 7811$ K when using Eq. (6) in the calculation. If Eq. (7) is used instead, the resulting temperatures are $T_e = 14{,}002$ K and $T_g = 7798$ K, a difference of less than 0.3%. In the worst case the T_e discrepancy is 3.4% near the plasma tail, which is still well within the uncertainty in the calculation in any case.

To date we have found no record in the literature of non-LTE diagnostics performed on continuously maintained laser-produced plasmas. However, there are several reports of LSP diagnostics performed which make claims concerning LTE.

Generalov et al.[16] used Stark broadening of the H_β line to calculate electron number density in argon and xenon LSPs, and the Saha equation was used to calculate temperature assuming equilibrium. An approximate calculation of the maximum deviation of the electron temperature from the heavy particle temperature resulted in only a 6% deviation for argon, based on 100 W input laser power. The conclusion was that the LSP is in LTE to a first approximation. In that experiment, however, no attempt was made to determine the excitation temperature or to resolve the electron number density and temperature spatially. In addition, 100 W is not much laser power and might not have produced a high enough flux to generate a significant kinetic temperature deviation.

In another study of air LSPs, Keefer et al.[17] used the Fowler-Milne and absolute line intensity techniques to measure plasma temperature. Both of these techniques require that LTE exist to be accurate, and although the results are in agreement internally, LTE cannot be concluded from this experiment. Keefer does state that the presence of anomalous excited rotational structures in the molecular nitrogen ion found near the plasma boundaries may be due to non-LTE processes.

In a study of xenon LSPs, Cremers et al.[18] measured electron number density via Stark broadening and temperature via the Saha equation (assuming equilibrium). A Boltzmann plot was made after adding 66% krypton and using the krypton relative line intensities. The Boltzmann temperature agreed well with the Saha temperature, but as stated by the authors, "The quality is not sufficient to indicate positively that the [Boltzmann] plot is linear."[18] This along with no Abel inversion of the data, the comparison of two differently composed plasmas, and the assumption of equilibrium in the use of the Saha equation prevent a confirmation of LTE in these LSPs.

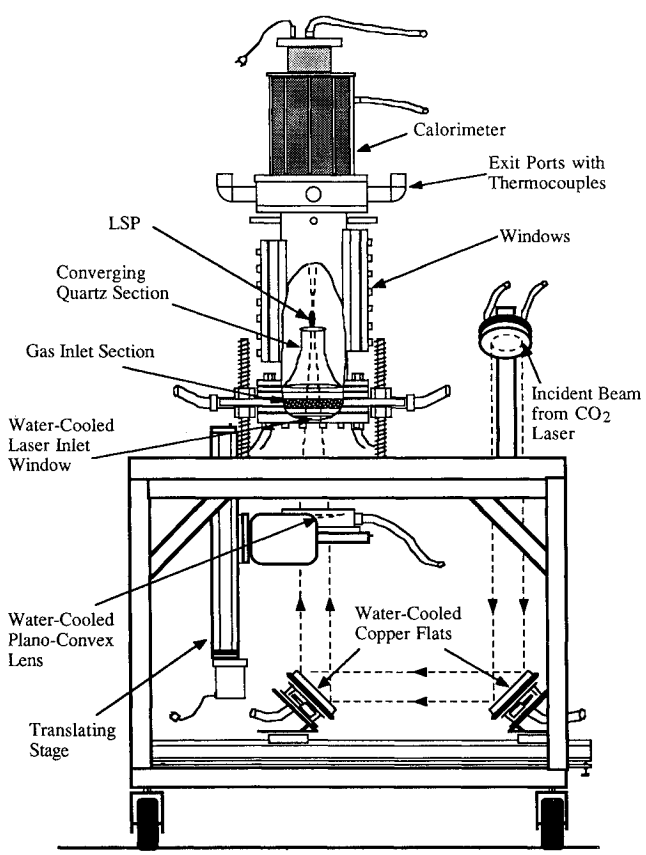

Fig. 1 Schematic of the LSP absorption chamber.

Experiments

A 10 kW Avco-Everett HPL-10 continuous-wave CO_2 laser with an output wavelength of 10.6 μ is used in this investigation. The unstable resonator output produces an annular beam with a 74-mm o.d. and a 50-mm i.d. Figure 1 is a schematic of the absorption chamber test stand. The stand supports the laser absorption chamber and all of the beam steering optics.

The direction of beam propagation is into the page in Fig. 1. The beam steering optics consist of three water-cooled, flat copper turning mirrors, and a zinc selenide (ZnSe) focusing lens. There is also a ZnSe inlet window mounted at the bottom of the absorption chamber. The lens has a focal length of 305 mm, resulting in an f/4.1 beam focusing geometry.

Because axial as well as radial spectroscopic measurements are made in this investigation, special attention is paid to the collection optics. The spectrometer and detector combination is capable of gathering both spectral and radial information simultaneously, but axial measurements must be made sequen-

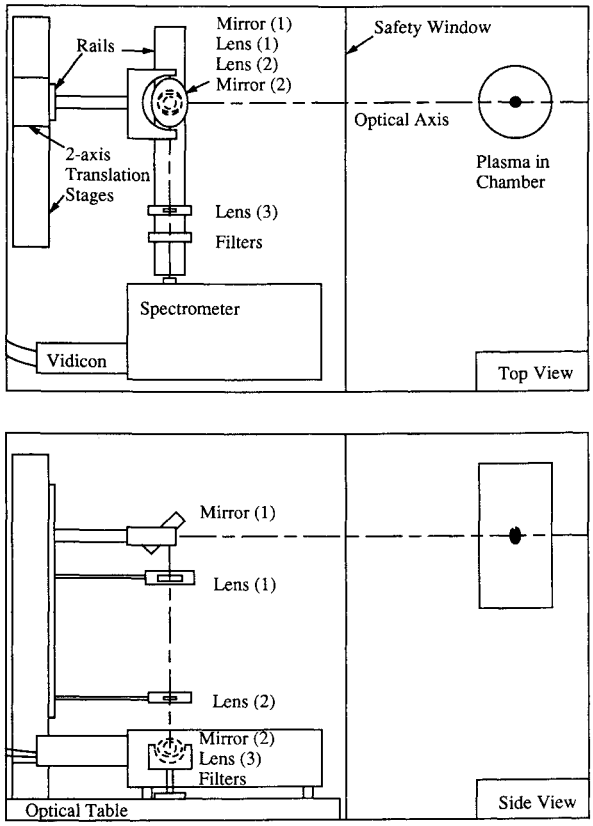

Fig. 2 Schematic of the LSP emission collection optics.

tially by traversing the collection optics vertically through the LSP domain. The difficulty in designing an optical system like this is to maintain a focused image on the spectrometer entrance slit while the overall optical path length changes as the optics are traversed vertically.

Figure 2 is a two-view schematic showing the relative positions of the plasma and laser absorption chamber, the collection optics, and the spectrometer. The first lens is a 121-mm focal length, 2-in.-diam achromat to which a second achromat of 65-mm focal length and 25-mm diameter is matched so that collimated light results as output from the lens combination. This matching permits these first three optical components to be traversed vertically without altering the final image location.

The second coated aluminum mirror accepts the collimated light and turns the signal parallel to the optical table and flips the plasma image to horizontal as well. The third and last achromatic lens images the plasma onto the vertically oriented spectrometer entrance slit. With a 121-mm focal length and 24-mm diameter, this last lens automatically stops down the light so that f/5 focusing results, thus matching the spectrometer f-number for all wavelengths studied. The first lens is approximately 1.11 m from the plasma centerline resulting in an overall magnification of $(4.47)^{-1}$.

An Instruments S.A., Inc. model HR-321 (321-mm focal length) coma corrected, Czerny-Turner configuration spectrometer is used in this investigation. A 1200-g/mm holographic diffraction grating is used in the spectrometer, providing both high resolution and a bandpass large enough for these experiments. The entrance slit of the spectrometer is 8 mm high and 0.025 mm wide. This results in an axial spatial resolution of 0.11 mm given the external magnification of $(4.47)^{-1}$.

The detector is an EG&G PARC model 1254 intensified vidicon array. It is mounted to the spectrometer housing at the exit focal plane. The two-dimensional array measures 500 pixels in the spectral dimension and 512 pixels in the spatial direction. Because the plasma image is turned horizontal by the collection optics, the vertical entrance slit of the spectrometer resolves lateral position in the LSP. Vidicon control software allows pixel grouping, and in this experiment five rows of pixels are grouped to represent a given lateral location. With each pixel measuring 25 μ in size, and external magnification being 4.47 (going backwards to the plasma object), lateral spatial resolution is

$$(5 \text{ pixels})(0.025 \text{ mm/pixel})(4.47) = 0.5588 \text{ mm} \tag{8}$$

The linear dispersion is nominally 2.2 nm/mm at approximately 550 nm for this grating-spectrometer combination. The actual spectral resolution of the vidicon detector array is determined more precisely for each wavelength of interest by scanning the emission of well-characterized wavelength standard lamps. Spectral resolution ranges from 0.55 to 0.63 Å per pixel over the emission lines measured in this experiment.

The detector is controlled and scanned by an EG&G PARC model 1216 detector controller, which is in turn controlled by an EG&G PARC model 1460 Optical Multichannel Analyzer (OMA III) console. The detector is calibrated for absolute spectral radiance by comparing plasma emission to the emission of an Optronic Laboratories, Inc. model 453-1 calibrated source of spectral radiance.

The selection procedure for the neutral and ionic argon lines is as follows. For each system (neutral or ionic) a high-energy line and a low-energy line must be chosen. Within the high- or low-energy range, only lines with relatively well-known spontaneous emission coefficients are considered [± 25% uncertainty or better on the National Bureau of Standards (NBS) scale[10]]. From preliminary plasma studies, emission lines strong enough to be easily measured are determined, as are lines which appear to be isolated from other lines. Tabulated argon spectra are then checked to make sure no hidden interference exists in the lines remaining under consideration.[10] Strength of self-absorption is then checked using oscillator strength considerations, and the lines most free of this drawback are chosen for study.

Table 2 contains the pertinent information on the argon lines chosen for study. The spontaneous emission coefficients shown are not the NBS values, in general. Updated values for the neutral lines are taken from more recent literature considering the effects of non-LTE on measured transition probabilities.[19] The ion data are those of Olsen[20] and fall within the stated uncertainty of the NBS values.

Hydrogen is introduced into the primary argon flow in an amount small enough to have no effect on the plasma thermodynamic state. In this experiment 7 mg/s of hydrogen are added to 25 g/s of argon, which corresponds to about 1/2% hydrogen by volume. The strength of argon emission lines measured with and without this trace hydrogen flow are the same, thus justifying the addition of this diagnostic seed.

Data Analysis

The main functions of the initial data reduction are to smooth the spectral profiles, determine and subtract the background signal, calibrate the net spectral profile, and to integrate the line and adjacent continuum signals. Integration is not performed on the hydrogen line because it is the spectral information which is required for electron number density determination, not total intensity.

Abel inversion is a mathematical procedure for calculating the reconstruction of a circularly symmetric two-dimensional

Table 2 Spectroscopic data

λ, Å	Species	E_m, cm^{-1} upper	g_m	A_{mn}(10^6 s^{-1})	A_{mn}(10^6 s^{-1}) (NBS)
7147	neutral	107132	3	0.462 ± 4%	0.650 ± 25%
6752	neutral	118907	5	3.015 ± 10%	2.01 ± 25%
4658	ionic	159706	2	69.5 ± 10%	81.0 ± 25%
4610	ionic	170530	8	90.6 ± 5%	91.0 ± 25%

function from its lateral projection.[8] The lateral projection is usually the only type of information that can be measured in an emission spectroscopic experiment. It is then necessary to perform an Abel inversion to recover radial information, which in a circularly symmetric plasma represents a complete spatial description at a given axial location.

The integral transform method chosen for this investigation is based on the work of Smith et al.[21] and has several advantages that make it more attractive than other Abel inversion techniques. A discrete fast Fourier transform is taken of the original lateral profile and a user specified low-pass filter is applied in Fourier space. A procedure for determining the best axis of symmetry is included in the method, and the Abel inversion is reformulated so that an inverse Hankel transform is used to reconstruct the radial emission profile. A detailed description of the reformulation and application of Abel inversion by integral transforms is found in the article by Smith et al.[21]

The result of the initial data reduction is a complete two-dimensional (radial and axial) set of emission coefficients for four integrated argon lines and the spectral profile of H_α. The initial data analysis includes calculating the population of the upper electronic level involved in each of the four argon line transitions.

The radial emission coefficient for an argon line transition is related to the population of the upper level of the transition, n_m, as follows[8]:

$$n_m = \frac{4\pi\lambda_{mn}\epsilon(r)_L}{hcA_{mn}} \tag{9}$$

where λ_{mn} (cm) is the center wavelength of the line transition, c (cm/s) is the speed of light, and A_{mn} (1/s) is Einstein's coefficient for spontaneous emission from level m to level n.

The populations of the upper levels are used to calculate plasma temperature and composition based on the assumption LTE. This relatively simple analysis has enjoyed great popularity. For example see Keefer et al.[22] for both absolute and relative line intensity temperature determination techniques, or Drellishak et al.[23] for LTE argon compositions and thermodynamic properties. It will be shown, however, that non-LTE analysis is required for the purpose of determining the complete thermodynamic state of the LSP studied in this investigation.

Preliminary analysis also involves using the H_α spectral profile to determine n_e at each of the points in the two-dimensional plasma domain. The unified theory of hydrogen line Stark broadening[24] is employed in a computer program written by Chan and Montaser[25] to calculate n_e from the spectral shape of H_α. The program was written in BASIC for execution on IBM compatible personal computers, but has been converted to FORTRAN by the authors for execution on the Convex mainframe computer on the University of Illinois campus. The original program was provided by Professor Alexander Scheeline of the University of Illinois at Urbana-Champaign Chemistry Department.[26]

The goal of non-LTE data analysis is to determine, independent of an explicit LTE assumption, the kinetic temperatures of the electrons and heavy species, the total excitation temperatures of neutral and ionic argon, and the number densities of the neutral and ionic species. The electron number density determined from the Stark broadened H_α line shape is taken as a quantity known independent of an LTE assumption.

Based on the critical electron number density criteria of Drawin and Griem shown earlier, it is assumed that n_a can be approximated from the Boltzmann relation using the LTE temperature in the exponential term.

$$n_a = \left(\frac{n_m}{g_m}\right)_{7147} Z_{exa}(T_{\mathrm{LTE}}) \exp\left[\frac{E_m}{k_b T_{\mathrm{LTE}}}\right] \tag{10}$$

The 7147-Å line is used rather than the 6753-Å line because the uncertainty in the spontaneous emission coefficient is lower for the 7147-Å line. In addition, the total excitation temperatures are assumed equal to the LTE temperatures corresponding to the respective neutral and ionic line emissions. The ion number density is assumed equal to the electron number density, based on plasma quasineutrality and first-degree ionization dominance.

There are then two unknowns which must be calculated, T_e and T_g, and so two equations are required to arrive at a unique solution. The following equations are assumed valid for the LSP studied in this investigation. The first is the gas equation of state:

$$P = k_b[n_e T_e + (n_a + n_i)T_g](1 - P_c^{DH}) \tag{11}$$

where P_c^{DH} is the Debye-Huckel pressure correction term. The second is the non-LTE ionization: See Eq. (6).

The assumption regarding Boltzmann equilibrium is not necessary to determine the ion density because it is assumed equivalent to the measured electron number density. However, it is an interesting check on the assumption to carry out the calculation and to compare the resultant ion density to the electron density. This has been done and the results to be shown indicate a very favorable comparison.

Equations (6), (10), and (11) are used to solve for T_e, T_g, and n_a in an iterative solution algorithm. The logic is as follows:

1) Read the values of n_e, $T_{\mathrm{LTE},7147}$, $T_{\mathrm{LTE},4610}$, and $(n_m/g_m)_{7147}$ from preliminary results data files. Set $T_{exa} = T_{\mathrm{LTE},7147}$, $T_{exi} = T_{\mathrm{LTE},4610}$, and $n_i = n_e$.

2) Make an initial estimate for n_a from Eq. (10) with $Z_{exa} = 1$.

3) Make an initial estimate of electron kinetic temperature, T_e = 16,000 K, and an initial estimate of the heavy kinetic temperature, T_g = 5000 K.

4) Calculate the plasma Debye length and the lowered ionization potential.

5) Calculate the partition functions.

6) Calculate n_a from Eq. (10) with the new lowered ionization potential and partition function.

7) Calculate T_e from Eq. (6), rearranged so that the new T_e comes from the electron translational partition function and appears as a function of the T_e from the previous iteration.

8) Calculate n_i from quasineutrality.

9) Calculate the Debye-Huckel pressure correction.

10) Calculate the system pressure from Eq. (11). If the calculated system pressure is not in close agreement with the known system pressure, then T_e is under-relaxed so that:

$$T_e = T_e' + R(T_{e,\mathrm{calc}} - T_e') \tag{12}$$

T_g is then incremented, and the procedure is repeated starting at step 4.

T_g is incremented in steps of 210 K until the algorithm overshoots the solution. The increment is then halved and the sign reversed so that the solution is approached from the other side of the root. This halving and reversing procedure is continued until the calculated pressure agrees closely with the known system pressure.

Results and Discussion

There are two main bodies of results which are discussed. The initial results include the argon line emission coefficients, electron number density from H_α, and LTE temperature and composition. The final non-LTE results include the kinetic temperatures T_e and T_g. Additional comparisons are made to the results of the LTE numerical model of Eguiguren.[7] The LSP conditions for which all analyses are based are 5 kW incident laser power, an f/4 beam focusing geometry, and 13.8 kg/m^{2}s incident argon mass flux. This mass flux corresponds to a flow velocity of 8.5 m/s at 1 atm system pressure.

Contour plots of the emission coefficient for the argon neutral line at 7147 Å and the argon ion line at 4160 Å are shown in Fig. 3. The origin of the horizontal axis represents

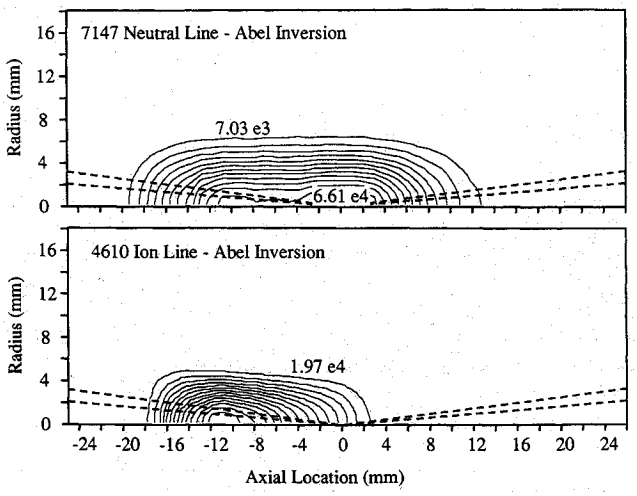

Fig. 3 Neutral and ion line emissivity contours (W/cm³sr); the contour interval is 5.37 *e*3 in the upper plot and 1.97 *e*4 in the lower plot; the central contour in the lower plot is 2.76 *e*5.

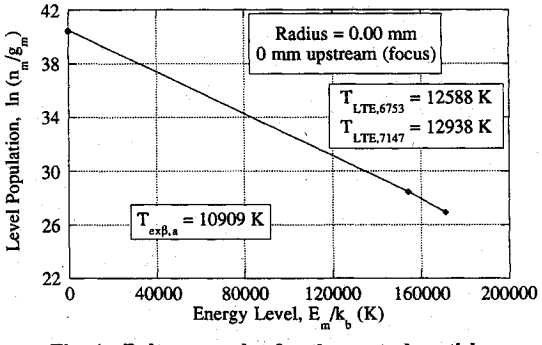

Fig. 4 Boltzmann plot for the neutral particle.

the laser focus, and the dashed lines show the path of the laser beam's inner and outer diameters through the plasma. The axes are scaled equally so that the actual proportions of the plasma emission are preserved. Both the gas flow and laser propagation are left to right in all contour plots.

Figure 4 contains a typical Boltzmann plot made using the populations of the upper levels in the 6753- and 7147-Å transitions in neutral argon. The axial location corresponds to the laser focus. The slope between the two upper-level points gives $T_{ex\beta,a}$. The slope between the lower energy level and the ground state corresponds to the LTE temperature of that level (also assumed to be T_{exa}). There are two points plotted at the ground state corresponding to natural $\log(n_a/Z_{exa})$ calculated from the LTE temperatures of the two upper energy level populations. These two ground-level densities are virtually indistinguishable on the Boltzmann plot, but small differences will be apparent when plotted on a linear ordinate.

The key feature of this Boltzmann plot is the near equivalence of the LTE temperatures and of the neutral densities predicted from these temperatures. The estimated error in the LTE temperature and neutral particle density determinations are $\pm 3\%$ and $\pm 9\%$, respectively.[27] $T_{ex\beta,a}$ does not agree as well with the LTE temperatures, but has a larger estimated error of $\pm 7\%$. More importantly, $T_{ex\beta,a}$ is lower than both LTE temperatures at every point in the LSP. This indicates that the error may be systematic in nature and possibly due to inaccuracy in the spontaneous emission coefficients for these argon lines. Although this is not necessarily true, it seems none the less that the neutral particle electronic system is in near-Boltzmann equilibrium, supporting the conclusion drawn from the Drawin and Griem criteria. The significance of this conclusion is that the neutral Boltzmann approximation used to calculate n_a from the 7147-Å line LTE temperature can be used with greater confidence, as can the assumption $T_{exa} = T_{LTE}$.

Figure 5 is a plot comparing the radial variation of neutral particle number density as calculated from the LTE analysis of the two neutral lines. The difference between the two densities not detectable on the Boltzmann plots is clearly visible on these linear ordinates. Again, the error in the determination from any one line is approximately $\pm 9\%$, which nearly encompasses the difference between the two lines at all locations. The neutral particle number density values determined from the 7147-Å line LTE analysis are the ones used in this investigation because the estimated error is slightly smaller due to a more precise spontaneous emission coefficient. There is currently no independent check on the validity of this neutral density determination method.

Figure 6 contains a Boltzmann plot made using the populations of the upper levels in the argon-ion transitions. Again, the LTE temperatures are very close together, even more so than for the neutral lines, and the ground-state populations predicted from each line are completely indistinguishable on the Boltzmann plot. The upper-level excitation temperature is generally quite higher than the LTE temperatures, but the estimated error is $\pm 12\%$ due to large uncertainty in the spontaneous emission coefficients and the relatively close spacing of the upper levels of the transitions as compared to the calculated excitation temperature.

A similar conclusion can be drawn from the ionic Boltzmann plots as is drawn from the preceding neutral plots. It is clear that the ion electronic system is in near-Boltzmann equilibrium, and that n_i can be determined with confidence from an LTE analysis of a single ion line. A comparison of the ion number density calculated in this way to the electron number density calculated from H_α Stark broadening confirms this claim.

Figure 7 is a typical plot comparing the radial variation of electron number density as calculated by three different methods. The H_α and ion LTE determinations agree quite well at all axial and radial locations, but the neutral LTE determination is clearly not in agreement. The agreement between two

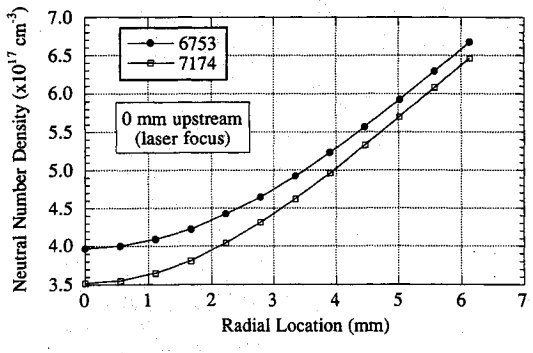

Fig. 5 Radial plot of neutral particle number density.

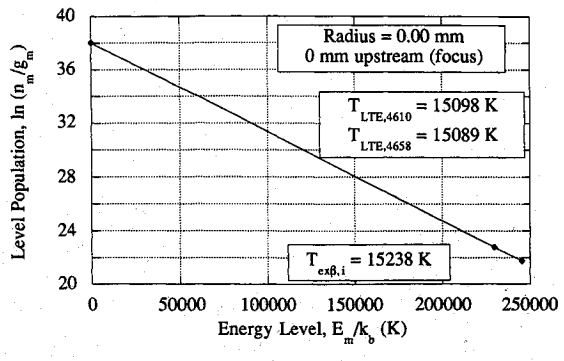

Fig. 6 Boltzmann plot for the ionic particle.

completely independent methods for determining electron number density tends to confirm the validity of both methods. The disagreement with a third method is also significant.

These results are important for two main reasons. First, it shows the large error that is introduced into the LSP electron number density determination if only LTE analysis of neutral argon emission is used. Second, for argon LSPs at atmospheric pressure it may be necessary to use only the LTE analysis of a suitable argon-ion line for electron number density determination (assuming quasineutrality with $n_e = n_i$). This eliminates the need for the somewhat involved calculations required for the undertaking of Stark broadening analysis. Also, the conditions on critical electron number density set out by Drawin[9] and Griem[8] [Eqs. (3) and (4), respectively] seem to be valid for this LSP as applied to the ions, and may be used as a check before using the ion LTE electron number density determination.

Figure 8 contains contour plots of electron number density as calculated by H_α Stark broadening analysis and by LTE analysis of the 4610-Å argon-ion line emission. Again, the agreement between these two contours is excellent. The radial and axial extent of the contour corresponding to 1.65×10^{17} cm^{-3} in the H_α plot is almost identical to the 1.6×10^{17} cm^{-3} contour on the ion LTE plot. The central contours near 2×10^{17} cm^{-3} on each plot also agree quite well. The estimated error in the H_α electron number density determination is $\pm 7\%$ (see Ref. 27). It is assumed that if the vidicon detector range allowed more extensive ion measurements, the results in the downstream region of the LSP would agree with the H_α results as well.

Figure 9 contains the contour plots of the electron and heavy particle kinetic temperatures. It is immediately obvious that significant kinetic nonequilibrium persists in this LSP, and that it is likely due to the presence of the laser beam. A temperature difference is driven by the continuous laser beam because

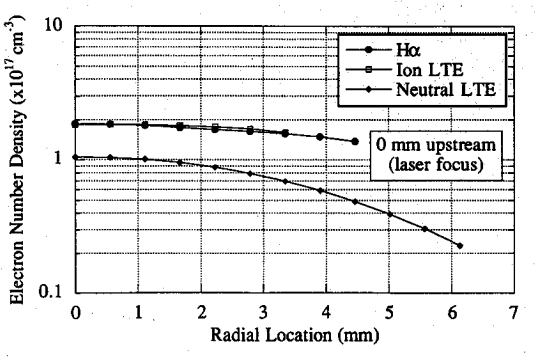

Fig. 7 Radial plot of electron number density.

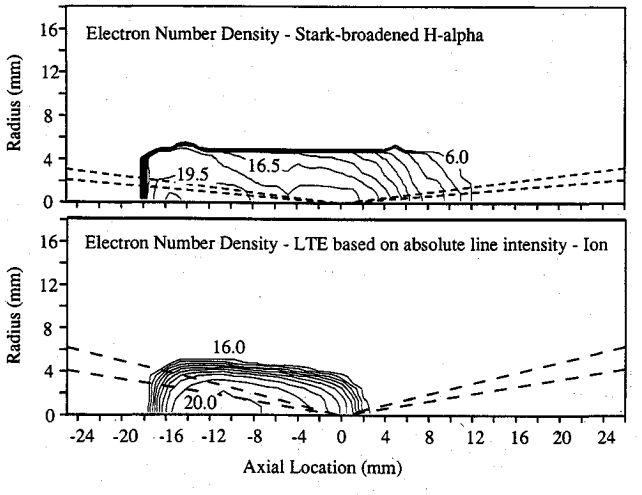

Fig. 8 Electron number density contours ($\times 10^{16}$ cm^{-3}); the contour interval is 1.5 *e*16 in the upper plot and 0.4 *e*16 in the lower plot.

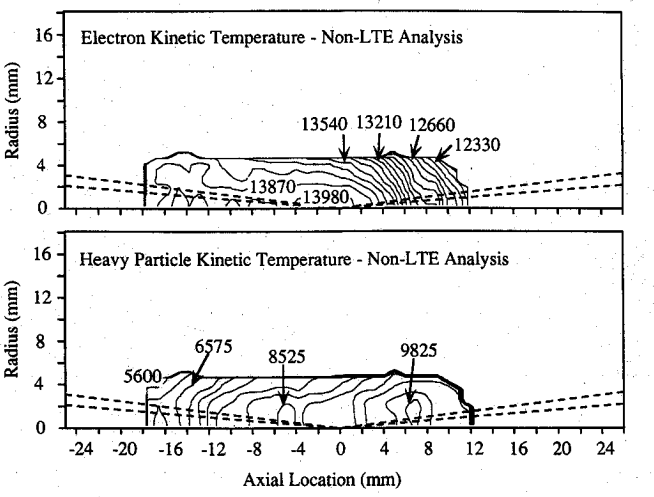

Fig. 9 Electron and heavy particle kinetic temperature contours; the contour interval is 110 K in the upper plot and 325 K in the lower plot.

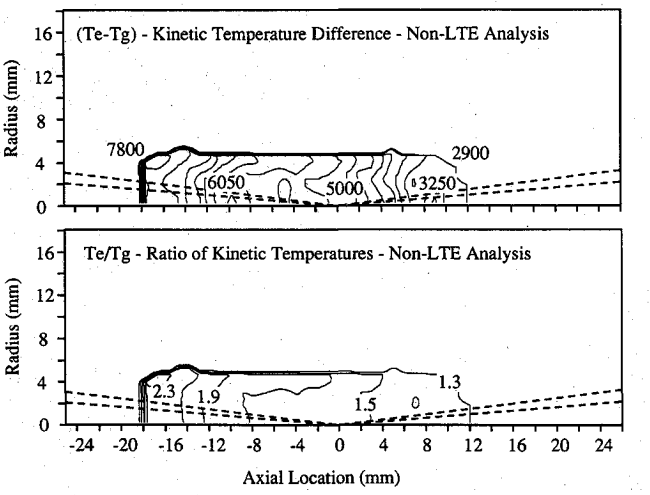

Fig. 10 Kinetic temperature difference and ratio contours; the contour interval is 350 K in the upper plot and 0.2 in the lower plot.

electrons absorb the laser photon energy during the inverse bremsstrahlung absorption process, and the heavy particles are heated secondarily through electron collisions. The difference contours ($T_e - T_g$) are shown in Fig. 10 along with the ratio contours (T_e/T_g). The kinetic nonequilibrium is greatest near the plasma front, where T_e is at its highest and T_g is at its lowest. This is because near the plasma front laser beam power absorption is at a maximum, and diminishes as the beam propagates downstream. Near the plasma tail the laser beam is severely weakened, and the heavy species have had a longer interaction time with the electrons so that the kinetic nonequilibrium is diminished. The estimated errors in the determination of T_e and T_g are $\pm 1\%$ and $\pm 10\%$, respectively.[27]

The numerical LSP model of Eguiguren[7] is based on the assumption of LTE. Figure 11 shows the temperature contours for the numerical model. The most striking observation is the LTE model's poor prediction of LSP position relative to the laser focus. The peak temperature is somewhat higher than even the electron kinetic temperature, but the predicted length of the plasma bounded by the 12,100 K contour is approximately the same for both contour plots.

It should be noted that the range of electron number density predicted by the LTE simulation is approximately the same as for the H_α determination. The electron number density is a key element in the calculation of the local laser beam absorption coefficient, and the overall plasma length is a factor in the total laser power absorption (or global absorption).

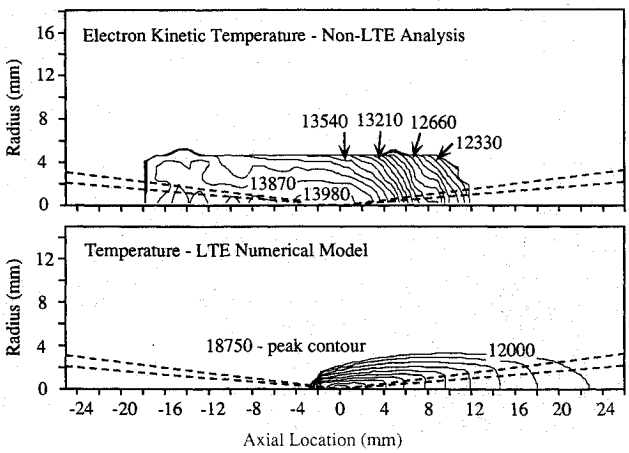

Fig. 11 Comparison to the LTE numerical model; the contour interval is 110 K in the upper plot and 750 K in the lower plot.

The laser beam absorption coefficient used in this investigation is due to Stallcop.[28] It is expressed as follows in units of m^{-1}:

$$\alpha_{IB} = \frac{256}{3}\sqrt{\frac{\pi}{3}}\,\pi^2(fsc)a_0\left(\frac{E_H}{hc}\right)^3\left(\frac{E_H}{k_b}\right)^{1/2} n_e^2\lambda^3(T_e)^{(-1/2)} \exp\left[\frac{hc}{\lambda k_b T_e}\right]\left[1-\exp\left(\frac{-hc}{k_b\lambda T_e}\right)\right]\left(\frac{hc}{\lambda k_b T_e}+g_{ff}\right) \tag{13}$$

This coefficient is calculated at every point in the LSP and the amount of beam power absorbed is calculated using a program written by Mertogul.[29] A small coefficient for electron-neutral IB is added to Eq. (13) and is curve fit from Geltman.[30] The total beam power absorption is calculated from the non-LTE analysis, the LTE numerical analysis, the LTE analysis of a single neutral emission line, and from calorimetric measurements of actual laser beam transmission through the LSP. Global absorption is calculated as the ratio of this absorbed power to the incident laser power and is expressed as a percentage of the incident power. This calculation yields 86 ± 6% (see Ref. 27) from the non-LTE analysis, 76 ± 4% (see Ref. 29) from calorimetry, 69% from the LTE model, and 43% from LTE emission diagnostics. The non-LTE analysis, calorimetric measurement, and LTE numerical analysis all agree fairly well, given the uncertainty of the measurements. The errors are expressed as absolute percent global absorption. The neutral line LTE analysis results in an extremely poor measure of global absorption due to the low electron number density associated with it.

The fact that the LTE numerical analysis results in a global absorption very close to that which is measured calorimetrically originally led to the belief that the physics of atmospheric pressure LSPs were being accurately modeled.[7] Based on the large kinetic nonequilibrium observed experimentally and the poor LTE model prediction of the LSP location, it is now clear that this is not the case, and that the numerical analysis is by no means guaranteed to produce accurate results if extended to LSP operating conditions beyond those available in the laboratory. It is clear that improved numerical modeling is required.

Conclusions

Nonlocal thermodynamic equilibrium is a significant effect in laboratory laser-sustained argon plasmas. The most important factor is kinetic nonequilibrium between the electrons and the heavy particles. The greatest deviation between kinetic temperatures occurs near the plasma front, where the laser power absorption is highest. The beam is attenuated as it passes through the plasma and kinetic nonequilibrium is not as severe in the plasma tail.

Nonequilibrium between the electron kinetic temperature and the electronic excitation temperatures is another significant effect in this LSP. Often the electron kinetic temperature is assumed to be equivalent to the upper-level excitation temperature of the neutral particles. This is a very poor approximation in this LSP because $T_{ex\beta,a}$ is typically 3000–5000 K lower than the electron kinetic temperature. In addition, $T_{ex\beta,a}$ is subject to large errors due both to uncertainties in the spontaneous emission coefficients and systematic error associated with the accuracy of these coefficients.

The ion number density determined from an LTE analysis of an ion upper energy level population in this LSP agrees extremely well with the electron number density determined through a Stark broadening analysis of the hydrogen Balmer series alpha line spectral profile. This result validates the ion LTE analysis as a means for determining electron number density in this LSP. The critical electron number density criteria for Boltzmann equilibrium due to Drawin[9] and Griem[8] seem to be valid indicators for this LSP. The result for the ion electronic system is especially convincing.

Some question remains concerning the values for the spontaneous emission coefficients used for argon line transitions. The values used for neutral argon in this investigation do not agree well with the more commonly accepted National Institute of Standards and Technology (NIST) values.[31] However, use of the NIST values changes only the degree of the kinetic nonequilibrium calculated. NIST values of the neutral argon spontaneous emission coefficient lead to an even higher prediction of neutral particle number density, thus the heavy particle kinetic temperature is lowered even further. More recent values for the argon ion spontaneous emission coefficients[32] have better agreement with the values used in this investigation, almost to within the stated uncertainties.

Future numerical modeling of laser-sustained plasmas should include non-LTE effects. Based on this investigation, the most important effect to include is kinetic nonequilibrium. Also of value would be the inclusion of some method for tracking optically thick radiative transport through the plasma. Current LTE models use experimentally determined values of radiative conductivity which may or may not be applicable to a general plasma geometry.

These improvements in a numerical model may help to better predict LSP position relative to the laser focus. This investigation has shown how kinetic nonequilibrium affects the relative plasma particle number densities. Increased electron and ion number densities are possible in regions near the plasma front due to the decreased partial pressure of the neutral particles, thus the laser power absorption coefficient is larger. The overall effect is the movement of the plasma front farther upstream of the laser focus than it would be if kinetic equilibrium were held. In addition, if the radiative conductivity used by the current LTE numerical model is too low, then the radiative/conductive preheating of the cold inlet gas is underestimated. This would have the effect of pushing the plasma front back closer to the laser focus.

In laser-sustained plasmas at pressures above one atmosphere, LTE is more likely to hold due to increased collisional energy transfer. This effect was noted by Jeng et al.[33] in comparisons between experimental and numerical results for argon LSPs at pressures of 2.0–3.0 atm. Although both the experiments and the model relied on the LTE assumption, positional inaccuracy did not appear to be a problem. This could be due to LTE persisting at these elevated pressures, because as Jeng et al. noted, at pressures below 2 atm the agreement between model and experimental results began to break down. A future experiment in which non-LTE diagnostics and LTE modeling are applied to LSPs at a range of pressures above one atmosphere could help to describe the transition from LTE to non-LTE in laser-sustained plasmas.

Acknowledgments

This research was supported by the Air Force Office of Scientific Research under grant AFOSR 89-0274; Mitat Birkan

was the program manager. The authors thank Jyotirmoy Mazumder, the grant coprincipal investigator, for his advice and insight concerning laser-gas interactions. We also thank Thomas Eddy of the Idaho National Engineering Laboratory whose previous work performed in the field of non-LTE plasma diagnostics has been most helpful. Ayhan Mertogul and Materials Engineering Research Laboratory staff member Justin Koch have also been of great help in this investigation.

References

[1]Kantrowitz, A. R., "The Relevance of Space," *Astronautics and Aeronautics,* Vol. 9, Sept. 1971, p. 34.

[2]Kantrowitz, A. R., "Propulsion to Orbit by Ground-Based Lasers," *Astronautics and Aeronautics,* Vol. 10, May 1972, p. 74.

[3]Glumb, R. J., Ph.D. Thesis, Univ. of Illinois at Urbana-Champaign, Urbana, IL, June 1986.

[4]Welle, R., Keefer, D., and Peters, C., "Laser-Sustained Plasmas in Forced Argon Convective Flow, Part 1: Experimental Studies," *AIAA Journal,* Vol. 25, No. 8, 1987, p. 1093.

[5]Zerkle, D. K., Schwartz, S., Mertogul, A., Chen, X., Krier, H., and Mazumder, J., "Laser-Sustained Argon Plasmas for Thermal Rocket Propulsion," *Journal of Propulsion and Power,* Vol. 6, No. 1, 1990, pp. 38–45.

[6]Mertogul, A., Zerkle, D., and Krier, H., "Investigation of CO_2 Laser Sustained Hydrogen Plasmas," *Journal of Propulsion and Power,* Vol. 8, No. 5, 1992, pp. 1123–1125.

[7]Eguiguren, J. V., M.S. Thesis, Univ. of Illinois at Urbana-Champaign, Urbana, IL, 1989.

[8]Griem, H. R., *Plasma Spectroscopy,* McGraw-Hill, New York, 1964, pp. 150–158, 170–178.

[9]Drawin, H. W., *Zeitschrift für Physik,* Vol. 228, 1969, p. 99.

[10]Wiese, W. L., Smith, M. W., and Miles, B. M., "Atomic Transition Probabilities," National Bureau of Standards NSRDS-NBS 22, 1969.

[11]Eddy, T. L., and Sedghinasab, A., "The Type and Extent of Non-LTE in Argon Arcs at 0.1-10 Bar," *IEEE Transactions on Plasma Science,* Vol. 16, No. 4, 1988, p. 444.

[12]Eddy, T. L., "Low Pressure Plasma Diagnostic Methods," AIAA Paper 89-2830, July 1989.

[13]Cho, K. Y., Ph.D. Thesis, Georgia Inst. of Technology, Atlanta, GA, 1988.

[14]Potapov, A. V., "Chemical Equilibrium of Multitemperature Systems," *High Temperature,* Vol. 4, No. 1, 1966, pp. 48–51.

[15]Martinez-Sanchez, M., private communication, Massachusetts Inst. of Technology, May 1993.

[16]Generalov, N. A., Zimakov, V. P., Kozlov, G. I., Masyukov, V. A., and Raizer, Y. P., "Experimental Investigation of a Continuous Optical Discharge," *Soviet Physics—JETP (Zhurnal Eksperimental'noi i Teoretischeskoi Fiziki),* Vol. 34, No. 4, 1972, p. 763.

[17]Keefer, D. R., Henriksen, B. B., and Braerman, W. F., "Experimental Study of a Stationary Laser-Sustained Air Plasma," *Journal of Applied Physics,* Vol. 46, No. 3, 1975, p. 1080.

[18]Cremers, D. A., Archuleta, F. L., and Martinez, R. J., "Evaluation of the Continuous Optical Discharge for Spectrochemical Analysis," *Spectrochimica Acta,* Vol. 40B, No. 4, 1985, p. 665.

[19]Sedghinasab, A., Ph.D. Thesis, Georgia Inst. of Technology, Atlanta, GA, 1987.

[20]Olsen, H. N., *Journal of Quantitative Spectroscopy & Radiative Transfer,* Vol. 3, No. 1, 1963, p. 59.

[21]Smith, M. L., Keefer, D. R., and Sudharsanan, S. I., "Abel Inversion using Transform Techniques," *Journal of Quantitative Spectroscopy & Radiative Transfer,* Vol. 39, No. 5, 1988, pp. 367–373.

[22]Keefer, D., Sedghinasab, A., Wright, N., and Zhang, Q., "Laser Propulsion Using Free Electron Lasers," AIAA Paper 90-2636, July 1990.

[23]Drellishak, K. S., Knopp, C. F., and Cambel, A. B., "Partition Functions and Thermodynamic Properties of Argon Plasma," Arnold Engineering Development Center AEDC-TDR-63-146, Aug. 1963.

[24]Vidal, C. R., Cooper, J., and Smith, E. W., "Hydrogen Stark-Broadening Tables," *Astrophysical Journal Supplement Series,* Vol. 25, No. 214, 1973, pp. 37–136.

[25]Chan, S.-K., and Montaser, A., "Determination of Electron Number Density via Stark Broadening with an Improved Algorithm," *Spectrochimica Acta,* Vol. 44B, No. 2, 1989, pp. 175–184.

[26]Scheeline, A., private communication, 1990.

[27]Zerkle, D. K., Ph.D. Thesis, Univ. of Illinois at Urbana-Champaign, Urbana, IL, Oct. 1992.

[28]Stallcop, J. R., "Absorption Coefficient of a Hydrogen Plasma for Laser Radiation," *Journal of Plasma Physics,* Vol. 11, Pt. 1, Feb. 1974, pp. 111–129.

[29]Mertogul, A. E., Ph.D. Thesis, Univ. of Illinois at Urbana-Champaign, Urbana, IL, May 1993.

[30]Geltman, S., "Free-Free Radiation in Electron-Neutral Atom Collisions," *Journal of Quantitative Spectroscopy & Radiative Transfer,* Vol. 13, No. 7, 1973, pp. 601–613.

[31]Wiese, W. L., Brault, J. W., Danzmann, K., Helbig, V., and Kock, M., "Unified Set of Atomic Transition Probabilities for Neutral Argon," *Physical Review A,* Vol. 39, No. 5, 1989, pp. 2461–2471.

[32]Garcia, G., and Campos, J., *Journal of Quantitative Spectroscopy & Radiative Transfer,* Vol. 34, No. 1, 1985, p. 85.

[33]Jeng, S.-M., Keefer, D. R., Welle, R., and Peters, C., "Laser-Sustained Plasmas in Forced Argon Convective Flow, Part II: Numerical Studies," *AIAA Journal,* Vol. 25, No. 9, 1987, pp. 1224–1230.